Convergence Analysis in the L^∞ norm of the Numerical Gradient of the Shortley-Weller method

Jiwon Seo, Seung-yeal Ha, Chohong Min

May 5, 2017

Abstract

The Shortley-Weller method is a standard central finite-difference-method for solving the Poisson equation in irregular domains with Dirichlet boundary conditions. It is well known that the Shortley-Weller method produces second-order accurate solutions and it has been numerically observed that the solution gradients are also second-order accurate; a property known as super-convergence. The super-convergence was proved in the L^2 norm in [17]. In this article, we present a proof for the super-convergence in the L^∞ norm.

1 Introduction

We consider the Poisson equation in a smooth irregular domain Ω, with Dirichlet boundary condition on its boundary $\Gamma = \partial\Omega$:

$$\begin{cases} -\Delta u = f & \text{in} \quad \Omega \\ \quad\ u = g & \text{on} \quad \Gamma := \partial\Omega \end{cases}, \tag{1}$$

where f and g are given smooth functions.

The Shortley-Weller method is a standard central finite-difference-method for solving the boundary value problem (1). Its numerical solution is well known to be convergent to the analytic solution with the second order accuracy [3, 8]. For many physical problems of interest however, the gradient of the solution has more importance than the solution itself. For example, this is the case of incompressible fluids [2, 11, 15] and free boundary problems [4, 1], for which the accuracy of the gradient of (1) determines the accuracy of the solution. It is therefore an important topic to analyze the convergence of the numerical gradient of the Shortley-Weller method.

The numerical gradient has been observed to be second-order accurate in the L^∞ norm in numerical tests (e.g. [10]), but to this day the observation had not been confirmed by a mathematical proof. In the case of rectangular domains, the second-order convergence in the L^2 norm appears in a textbook [13], whereas in the case of polygonal domains, the 1.5 order of convergence in L^2 norm was proved by Li et al [9]. For arbitrary smooth domains, the super-convergence was proved in the L^2 norm in [17]. Recently Weynans [14] sketched a proof in the L^∞ norm based on the discrete Green function by Ciarlet [3, 8]. In particular, Weynans' proof is based on the commutativity between the discrete Laplacian and the gradient operators away from the boundary, as well as an error estimate near the boundary. However, although the conclusion in [14] is correct, many important details are omitted. For example, the numerical solution with error $O\left(h^3\right)$ does not necessarily implies a $O\left(h^2\right)$ error for the numerical gradient because of the division by a local step size $h_{i+\frac{1}{2},j}$ near the interface that can be much smaller than h. Likewise, the estimation of Green's function omits much details in its derivation. Instead of using the Green function, we focus on the commutative region of the discrete Laplacian and the discrete gradient, and we leverage the existing error analysis of our previous work [17] to present a rigorous and complete proof for the super-convergence in the L^∞ norm.

The rest of this paper after is organized as follows. In section 2, we review the notations and the existing error analysis, and we discuss the commutative region of the discrete gradient in section 3. Combining the commutativity and the existing error analysis, we provide a proof for the second-order convergence in the L^∞ norm in section 4.

2 Analysis of the numerical solution [17]

The domain $\Omega \subset \mathbb{R}^2$ is approximated by the set of grid nodes $\Omega^h := \Omega \cap (h\mathbb{Z})^2$, where $(h\mathbb{Z})^2$ denotes the set of grid nodes with uniform step size h. The boundary $\Gamma := \partial\Omega$ is approximated by Γ^h, the set of intersection points between Γ and the grid lines. As illustrated in figure 1, each grid node (x_i, y_j)

has four neighboring nodes in $\Omega^h \cup \Gamma^h$, which are denoted by $(x_{i\pm1}, y_j)$ and $(x_i, y_{j\pm1})$. Given a discrete function $v^h : \Omega^h \cup \Gamma^h \to \mathbb{R}$, Shortley and Weller [12] discretize the Laplacian $-\Delta^h v^h : \Omega^h \to \mathbb{R}$ by applying the standard central-finite-differences on each node and its adjacent neighbors as follows:

$$\begin{aligned}\Delta^h v^h_{ij} = &\left(\frac{v^h_{i+1,j} - v^h_{ij}}{h_{i+\frac{1}{2},j}} - \frac{v^h_{ij} - v^h_{i-1,j}}{h_{i-\frac{1}{2},j}} \right) \Big/ \frac{h_{i+\frac{1}{2},j} + h_{i-\frac{1}{2},j}}{2} \\ &+ \left(\frac{v^h_{i,j+1} - v^h_{ij}}{h_{i,j+\frac{1}{2}}} - \frac{v^h_{ij} - v^h_{i,j-1}}{h_{i,j-\frac{1}{2}}} \right) \Big/ \frac{h_{i,j+\frac{1}{2}} + h_{i,j-\frac{1}{2}}}{2}.\end{aligned}$$

The numerical approximation $u^h : \Omega^h \cup \Gamma^h \to \mathbb{R}$ for the Poisson problem (1) is the solution of the following linear system:

$$\begin{cases} -\Delta^h u^h = f & \text{in } \Omega^h, \\ \quad\;\; u^h = g & \text{on } \Gamma^h. \end{cases} \tag{2}$$

The consistency and the error vectors are important quantities in the error analysis and are defined as follows:

$$\begin{array}{rcll} \text{(consistency) } c^h & := & -\Delta^h u + \Delta u & \text{in } \;\Omega^h \\ \text{(error) } e^h & := & u^h - u & \text{in } \;\Omega^h \cup \Gamma^h \end{array} \tag{3}$$

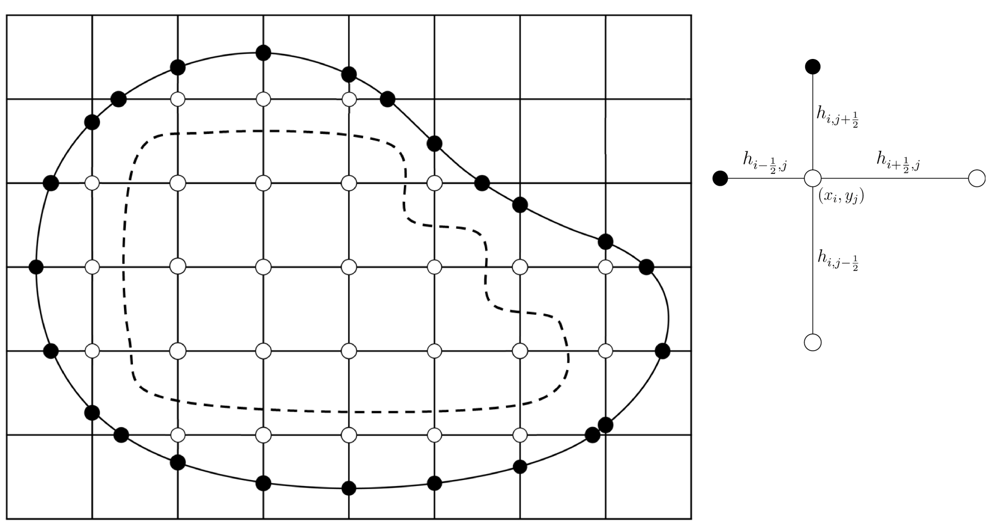

Figure 1: The nodes in Ω^h are marked with the symbol $\circ$, and the nodes in Γ^h with the symbol $\bullet$. The interior nodes in Ω^h_0 are enclosed in the dashed curve. Each grid node in Ω^h has four neighboring nodes in $\Omega^h \cup \Gamma^h$.

We recall the following results from the error analysis of [17] and refer the interested reader to [17] for the details.

Lemma 2.1. *Let e^h be a error defined by* (3)*. Then, e^h satisfies the following relation: $-\Delta^h e^h = c^h$ in Ω^h.*

Theorem 2.2. *(Comparison principle) If $v^h, w^h : \Omega^h \cup \Gamma^h \to \mathbb{R}$ satisfy $-\Delta^h v^h \leq -\Delta^h w^h$ in Ω^h and $v^h \leq w^h$ on Γ^h, then $v^h \leq w^h$ in Ω^h.*

Theorem 2.3. *(Refined error estimate) If h is sufficiently small, then there exists a constant $E = E(\Omega, u)$ such that for any $(x_i, y_j) \in \Omega^h$,*

$$\left|e_{ij}^h\right| \leq E(\Omega, u) h^2 \left(dist\left(\left(x_i, y_j\right), \Gamma^h\right) + \min\left\{h_{i\pm\frac{1}{2}.j}, h_{i,j\pm\frac{1}{2}}\right\}\right).$$

3 Commutativity of the discrete Laplace and Gradient operators for interior edges

For a discrete function v^h sampled at grid nodes, its discrete gradient values are calculated by central differencing and defined on the corresponding cell faces, following the Marker-and-Cell configuration [7]. For example, the derivative in the x-direction is calculated as follows:

$$\tilde{\Omega}^h := \left\{\left(x_{i+\frac{1}{2}}, y_j\right) | \left(x_i, y_j\right), \left(x_{i+1}, y_j\right) \in \Omega^h \cup \Gamma^h\right\},$$

$$\left(D_x^h v^h\right)_{i+\frac{1}{2},j} := \frac{v_{i+1,j}^h - v_{i,j}^h}{h_{i+\frac{1}{2},j}}, \text{ for each edge } \left(x_{i+\frac{1}{2}}, y_j\right) \in \tilde{\Omega}^h,$$

In this section, we discuss the commutativity of the two discrete operators Δ^h and D_x^h noting that the commutativity between Δ^h and D_y^h is similar. The calculation of $\left(\Delta^h\left(D_x^h v^h\right)\right)_{i+\frac{1}{2},j}$ requires four neighboring values of $\left(D_x^h v^h\right)_{i+\frac{1}{2},j}$, however the neighboring values may not exist near the boundary. As illustrated in figures 1 and 2, we define the set of interior nodes and the set of interior edges (faces) as:

$$\Omega_o^h := \left\{\left(x_i, y_j\right) | \left(x_{i\pm1}, y_j\right) \text{ and } \left(x_i, y_{j\pm1}\right) \in \Omega^h\right\}, \text{ and}$$

$$\tilde{\Omega}_o^h := \left\{\left(x_{i+\frac{1}{2}}, y_j\right) | \left(x_i, y_j\right) \text{ and } \left(x_{i+1}, y_j\right) \in \Omega_o^h\right\}.$$

Now we show the commutativity, $D_x^h \circ \Delta^h = \Delta^h \circ D_x^h$, for the interior edge set $\tilde{\Omega}_0^h$.

Theorem 3.1 (Commutativity)**.** *For any discrete function $v^h : \Omega^h \to \mathbb{R}$, $\left(\Delta^h \circ D_x^h\right) v^h$ and $\left(D_x^h \circ \Delta^h\right) v^h$ are well defined in $\tilde{\Omega}_o^h$, and they are equal.*

Proof. For each edge $\left(x_{i+\frac{1}{2}}, y_j\right) \in \tilde{\Omega}_o^h$, the grid nodes (x_i, y_j) and (x_{i+1}, y_j) belong to Ω_o^h, and all of their neighboring nodes belong to Ω^h. As illustrated in figures 1 and 2, there exist 8 neighboring nodes (denoted by the symbol $\circ$) around the edge and they are aligned with uniform step size h. The calculations of $\left(\Delta^h \left(D_x^h v^h\right)\right)_{i+\frac{1}{2},j}$ and $\left(D_x^h \left(\Delta^h v^h\right)\right)_{i+\frac{1}{2},j}$ are the same and expressed as a function of the 8 neighbors as follows:

$$\begin{aligned}
&\left(\Delta^h \left(D_x^h v^h\right)\right)_{i+\frac{1}{2},j} \\
&= \left(D_x^h \left(\Delta^h v^h\right)\right)_{i+\frac{1}{2},j} = \frac{1}{h^3} \left[\begin{array}{cccc} v_{i+2,j}^h & +v_{i+1,j+1}^h & +v_{i+1,j-1}^h & +5v_{i,j}^h \\ -v_{i-1,j}^h & -v_{i,j+1}^h & -v_{i,j-1}^h & -5v_{i+1,j}^h \end{array} \right].
\end{aligned}$$

□

4 Accuracy analysis of the discrete gradient

In this section, we prove the second-order accuracy of the solution's gradient in L^∞ norm. We first present several lemmas before we present our main results.

Lemma 4.1. *For any $(x_i, y_j) \in \Omega^h \cup \Gamma^h \setminus \Omega_\circ^h$, $dist\left(\left(x_i, y_j\right), \Gamma\right) \le h$.*

Proof. Since $(x_i, y_j) \notin \Omega_0^h$, either $(x_i, y_j) \in \Gamma^h$ or one of its neighboring nodes, at a distance at most h away, belong to Γ^h. Since $\Gamma^h \subset \Gamma$, in either case we have $\mathrm{dist}\left(\left(x_i, y_j\right), \Gamma\right) \le h$ □

Lemma 4.2. *The following estimate holds true:*

$$\left\| D_x^h e^h \right\|_{L^\infty\left(\tilde{\Omega}^h \setminus \tilde{\Omega}_0^h\right)} \le 2E \cdot h^2.$$

Proof. Since $\left(x_{i+\frac{1}{2}}, y_j\right) \notin \tilde{\Omega}_0^h$, either (x_i, y_j) or (x_{i+1}, y_j) belongs to $\Omega^h \cup \Gamma^h - \Omega_\circ^h$. By the above lemma, $\mathrm{dist}\left(\left(x_i, y_j\right), \Gamma\right) \le 2h$ and $\mathrm{dist}\left(\left(x_{i+1}, y_j\right), \Gamma\right) \le 2h$. Using theorem 2.3, we have

$$\begin{aligned}
\left| u_{i,j}^h - u\left(x_i, y_j\right) \right| &\le h_{i+\frac{1}{2},j} \cdot h^2 \cdot 2E, \text{ and} \\
\left| u_{i+1,j}^h - u\left(x_{i+1}, y_j\right) \right| &\le h_{i+\frac{1}{2},j} \cdot h^2 \cdot 2E.
\end{aligned}$$

Combining the two inequalities, we conclude that $\left\|D_x^h e^h\right\|_{L^\infty\left(\tilde{\Omega}^h\setminus\tilde{\Omega}_0^h\right)} \leq 2E\cdot h^2$. $\square$

Lemma 4.3. *Let $K := \frac{105}{4}\cdot\max_{\bar{\Omega},|\alpha|\leq 5}|\partial^\alpha u|$, then*

$$\left\|D_x^h c^h\right\|_{L^\infty\left(\tilde{\Omega}_0^h\right)} \leq K\cdot h^2.$$

Proof. Since $\left(x_{i+\frac{1}{2}}, y_j\right)\in\tilde{\Omega}_0^h$, (x_i, y_j) and (x_{i+1}, y_j) belongs to $\Omega_\circ^h$, and all of their adjacent nodes are aligned on the uniform grid. Thus $D_x^h c_{i+\frac{1}{2},j}^h$ is given as

$$\begin{aligned} D_x^h c_{i+\frac{1}{2},j}^h =& \frac{4u_{i+1,j}-u_{i+2,j}-u_{i,j}-u_{i+1,j+1}-u_{i+1,j-1}}{h^3}+\frac{\Delta u_{i+1,j}}{h} \\ &-\frac{4u_{i,j}-u_{i+1,j}-u_{i-1,j}-u_{i,j+1}-u_{i,j-1}}{h^3}-\frac{\Delta u_{i,j}}{h}. \end{aligned} \tag{4}$$

Substituting each term with its Taylor expansion at $\left(x_{i+\frac{1}{2}}, y_j\right)$ gives the following result. See the details in Appendix.

$$\begin{aligned} \left|D_x^h c_{i+\frac{1}{2},j}^h\right| &\leq \max_{\bar{\Omega},|\alpha|\leq 5}|\partial^\alpha u|\cdot\frac{h^2}{120}\left(2\cdot\left(\frac{3}{2}\right)^5+2\cdot\frac{5}{2^5}+4\cdot 6\cdot\left(\frac{1}{2}\right)^5+2\cdot 2\cdot\frac{5}{2}\right) \\ &= K\cdot h^2 \end{aligned}$$

$\square$

Lemma 4.4. *Consider the function $p^h:\tilde{\Omega}^h\to\mathbb{R}$ defined as $-\Delta^h p^h = 1$ in $\tilde{\Omega}_0^h$ and $p^h = 0$ on $\tilde{\Omega}^h\setminus\tilde{\Omega}_0^h$. There exists a constant $D = D(\Omega)$ such that $0\leq p^h\leq D$ in $\tilde{\Omega}$, whenever $h\leq\sqrt{\frac{6}{D}}$.*

Proof. Let $p(x)$ be the analytic solution of $-\Delta p = 2$ in Ω with $p = 0$ on Γ. Let us sample $p(x)$ in $\tilde{\Omega}^h$ and calculate $-\Delta^h p^h$ in $\tilde{\Omega}_0^h$. A simple Taylor expansion shows that

$$-\Delta^h p\left(x_{i+\frac{1}{2}}, y_j\right) = 2+\frac{h^2}{12}\left(\frac{\partial^4 p}{\partial x^4}(\xi_1, y_j)+\frac{\partial^4 p}{\partial x^4}\left(x_{i+\frac{1}{2}},\xi_2\right)\right),$$

for some $\xi_1\in(x_i, x_{i+1})$ and $\xi_2\in\left(y_{j-\frac{1}{2}}, y_{j+\frac{1}{2}}\right)$. Now, let $D = \max_{\bar{\Omega}}\left\{|p|, \left|\frac{\partial^4 p}{\partial x^4}\right|, \left|\frac{\partial^4 p}{\partial y^4}\right|\right\}$, then whenever $h\leq\sqrt{\frac{6}{D}}$,

$$\begin{array}{rcccl} -\Delta^h p^h = 1 & \leq 2-\frac{h^2}{12}2D\leq & -\Delta^h p & \text{in} & \tilde{\Omega}_0^h \\ p^h = 0 & \leq & p & \text{in} & \tilde{\Omega}^h\setminus\tilde{\Omega}_0^h. \end{array}$$

Then by the comparison principle 2.2, we have $0 \leq p^h \leq p \leq D$ in $\tilde{\Omega}^h$.

$\square$

Lemma 4.2 states that $D_x^h u^h$ is second-order accurate to $D_x^h u$ in $\tilde{\Omega}^h \setminus \tilde{\Omega}_\circ^h$. Now we investigate the excluded region $\tilde{\Omega}_\circ^h$ in the lemma to obtain our main theorem.

Theorem 4.5. *(Main theorem) Let $u(x,y)$ be the analytic solution of the Poisson problem in $\Omega \cup \Gamma$, and $u_{i,j}^h$ be the discrete solution in $\Omega^h \cup \Gamma^h$ obtained by the Shortley-Weller method, then there exists a constant $C = C(\Omega, u)$, independent of h, such that*

$$\left\| D_x^h u_{i+\frac{1}{2},j}^h - \frac{\partial u}{\partial x}\left(x_{i+\frac{1}{2}}, y_j\right) \right\|_{L^\infty\left(\tilde{\Omega}^h\right)} \leq C \cdot h^2.$$

Proof. Using the commutativity principle in $\tilde{\Omega}_0^h$, we have

$$-\Delta^h\left(D_x^h e^h\right) = D_x^h\left(-\Delta_x^h e^h\right) = D_x^h c^h \text{ in } \tilde{\Omega}_0^h.$$

Lemma 4.2 and lemma 4.3 state that

$$\begin{array}{rcll} -2E \cdot h^2 & \leq D_x^h e^h \leq & 2Eh^2 & \text{on} \quad \tilde{\Omega}^h - \tilde{\Omega}_0^h, \text{and} \\ -K \cdot h^2 & \leq D_x^h c^h \leq & Kh^2 & \text{in} \quad \tilde{\Omega}_0^h. \end{array}$$

Using the function p^h in lemma 4.4 and the commutativity principle, we have

$$\begin{array}{rcll} -\left(Kh^2p^h + 2Eh^2\right) \leq & D_x^h e^h & \leq Kh^2p^h + 2Eh^2 & \text{on} \quad \tilde{\Omega}^h - \tilde{\Omega}_0^h \\ -\Delta^h\left(-\left(Kh^2p^h + 2Eh^2\right)\right) & \leq -\Delta^h\left(D_x^h e^h\right) \leq & -\Delta^h\left(Kh^2p^h + 2Eh^2\right) & \text{in} \quad \tilde{\Omega}_0^h. \end{array}$$

Applying the comparison principle, we obtain:

$$-\left(Kh^2p^h + 2Eh^2\right) \leq D_x^h e^h \leq Kh^2p^h + 2Eh^2 \text{ in } \tilde{\Omega}^h,$$

while invoking lemma 4.4 gives

$$\left\|D_x^h e^h\right\|_{L^\infty\left(\tilde{\Omega}^h\right)} \leq h^2\left(K \cdot D + 2E\right).$$

The error of the central finite difference is bounded as follows:

$$\left| \frac{u\left(x_{i+1}, y_j\right) - u\left(x_i, y_j\right)}{h_{i+\frac{1}{2},j}} - \frac{\partial u}{\partial x}\left(x_{i+\frac{1}{2}}, y_j\right) \right| \leq \frac{h_{i+\frac{1}{2},j}^2}{24} \max_{\bar{\Omega}} \left| \frac{\partial^3 u}{\partial x^3} \right|.$$

Finally, by the triangle inequality, we have

$$\left\| D_x^h u_{i+\frac{1}{2},j}^h - \frac{\partial u}{\partial x}\left(x_{i+\frac{1}{2}}, y_j\right)\right\| \leq h^2 \left(K \cdot D + 2E + \frac{1}{24} \max_{\bar{\Omega}} \left| \frac{\partial^3 u}{\partial x^3} \right| \right).$$

$\square$

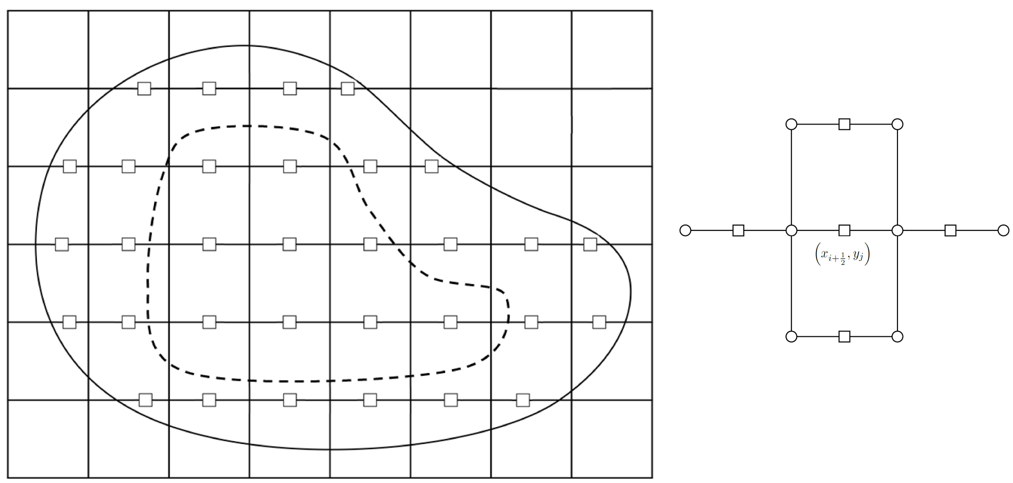

Figure 2: The edges in $\tilde{\Omega}^h$ are marked with the symbol $\square$, and the interior edges are enclosed by the dashed curve. Each interior edge $\left(x_{i+\frac{1}{2}}, y_j\right)$ has 8 neighboring nodes (marked with the symbol $\circ$) in Ω^h.

5 Analysis in three spatial dimensions

In the previous sections, we have analyzed the convergence in two spatial dimensions. Since the Shortley-Weller method follows a dimension-by-dimension approach, the analysis in three spatial dimensions is similar, except for a few exceptions that we detail next.

The domain $\Omega \subset \mathbb{R}^3$ is approximated by the set of grid nodes $\Omega^h := \Omega \cap (h\mathbb{Z})^3$ and Γ^h, i.e. the intersection of Γ and the grid lines of $(h\mathbb{Z})^3$. The discrete Laplacian is defined as:

$$\begin{aligned}\Delta^h v_{ijk}^h = & \left(\frac{v_{i+1,j,k}^h - v_{ijk}^h}{h_{i+\frac{1}{2},j,k}} - \frac{v_{ijk}^h - v_{i-1,j,k}^h}{h_{i-\frac{1}{2},j,k}}\right) / \frac{h_{i+\frac{1}{2},j,k} + h_{i-\frac{1}{2},j,k}}{2} \\ & + \left(\frac{v_{i,j+1,k}^h - v_{ijk}^h}{h_{i,j+\frac{1}{2},k}} - \frac{v_{ijk}^h - v_{i,j-1,k}^h}{h_{i,j-\frac{1}{2},k}}\right) / \frac{h_{i,j+\frac{1}{2},k} + h_{i,j-\frac{1}{2},k}}{2} \\ & + \left(\frac{v_{i,j,k+1}^h - v_{ijk}^h}{h_{i,j,k+\frac{1}{2}}} - \frac{v_{ijk}^h - v_{i,j,k-1}^h}{h_{i,j,k-\frac{1}{2}}}\right) / \frac{h_{i,j,k+\frac{1}{2}} + h_{i,j,k-\frac{1}{2}}}{2},\end{aligned}$$

and we can derive the corresponding main theorem, as in the previous sections.

Theorem 5.1. *(Main theorem in $\mathbb{R}^3$) Let $u(x, y, z)$ be the analytic solution of the Poisson problem in $\Omega \cup \Gamma$, and $u_{i,j,k}^h$ be the discrete solution in $\Omega^h \cup \Gamma^h$ obtained by the Shortley-Weller method, then there exists a constant $C' = C'(\Omega, u)$, independent of h, such that*

$$\left\| D_x^h u_{i+\frac{1}{2},j,k}^h - \frac{\partial u}{\partial x}\left(x_{i+\frac{1}{2}}, y_j, z_k\right)\right\|_{L^\infty\left(\tilde{\Omega}^h\right)} \leq C' \cdot h^2.$$

The only notable difference is the constant in lemma 4.3.

Lemma 5.2. *Let $K' := \frac{257}{30} \cdot \max_{\bar{\Omega}, |\alpha| \leq 5} |\partial^\alpha u|$, then*

$$\left\| D_x^h c^h \right\|_{L^\infty\left(\tilde{\Omega}_0^h\right)} \leq K' \cdot h^2.$$

6 Conclusion

We have presented a formal mathematical proof that the discrete gradient obtained from the Shortley-Weller method is second-order accurate in the L^∞ norm. This work can thus provide useful guidelines on how to compute the gradient of the Poisson solution at every grid nodes. In turn, this can be used in a plethora of applications in computational fluid dynamics and free boundary problems where the gradient drives the accuracy of the simulations.

Elliptic problems exhibit a strong dependence of the solution from any grid location to the entire region in space. As a result, an adaptive grid with finer resolution in some regions is not as efficient in elliptic problems as they are in hyperbolic and parabolic problems. Finite difference methods are simple to implement and easy to use, and are therefore very attractive for solving elliptic problems. However, formal proof of accuracy analysis are rare, as opposed to what is found in the finite element community.

We hope this work will incite other researchers to attempt many unsolved problems of finite difference methods. For example, we list below two open problems that, to the best of our knowledge, are still unsolved. In his seminal work [6], Gustafsson conjectured that only modified-ILU preconditioner decreases the condition number by one less order than the other ILU-type preconditioners. Gustafsson's conjecture was proved in the case of a symmetric finite difference method [16], but not in the case of the Shortley-Weller method. [5] introduced a finite difference method for solving fluid-solid-interaction, and recently proved that the solid velocity is at least first-order accurate [18]. Numerical results for the solid velocity however strongly suggests that second-order convergence is obtained, a proof of which has not yet been provided.

Appendix. Detailed calculations in Lemma 4.3

In this section, we provide detailed calculations that lead to the estimate $\left\|D_x^h c^h\right\|_{L^\infty\left(\tilde{\Omega}_o^h\right)} \leq \frac{105}{4} \max_{\tilde{\Omega},|\alpha\leq 5|} |\partial^\alpha u| \cdot h^2$ in lemma 4.3.

Using the Taylor series of $u\left(x,y\right)$ at $\left(x_{i+\frac{1}{2}}, y_j\right)$, the terms that sum up $D_x^h c^h$ in (4) are expanded. For notational conveniences, the local coordinates centered at $\left(x_{i+\frac{1}{2}}, y_j\right)$ are used in the calculations. For example, $u_{i+1,j+1}$ is denoted by $u\left(\frac{h}{2}, h\right)$. The Taylor expansions are listed below with remainders.

$$u\left(\pm\tfrac{3h}{2},0\right) = u \pm \tfrac{3h}{2}u_x + \tfrac{9h^2}{8}u_{xx} \pm \tfrac{9h^3}{16}u_{xxx} + \tfrac{27h^4}{128}u_{xxxx} \pm \tfrac{81h^5}{1280}u_{xxxxx}\left(\xi_1^\pm,0\right)$$
$$u\left(\pm\tfrac{h}{2},0\right) = u \pm \tfrac{h}{2}u_x + \tfrac{h^2}{8}u_{xx} \pm \tfrac{h^3}{48}u_{xxx} + \tfrac{h^4}{384}u_{xxxx} \pm \tfrac{h^5}{3840}u_{xxxxx}\left(\xi_2^\pm,0\right)$$

$$\Delta u\left(\pm\tfrac{h}{2},0\right) = \Delta u \pm \tfrac{h}{2}\left(u_{xxx}+u_{xyy}\right) + \tfrac{h^2}{8}\left(u_{xxxx}+u_{xxyy}\right) \pm \tfrac{h^3}{48}\left(u_{xxxxx}+u_{xxxyy}\right)\left(\xi_4^\pm,0\right)$$

$$
\begin{aligned}
u\left(\pm\tfrac{h}{2},\pm h\right) = u &+ \left(\pm\tfrac{h}{2}\right)u_x + \left(\pm\tfrac{h}{2}\right)^2 u_{xx} + \left(\pm\tfrac{h}{2}\right)^3 \tfrac{u_{xxx}}{3!} + \left(\pm\tfrac{h}{2}\right)^4 \tfrac{u_{xxxx}}{4!} + \left(\pm\tfrac{h}{2}\right)^5 \tfrac{u_{xxxxx}}{5!}\left(\tfrac{1}{2}\xi_3^{\pm,\pm},\xi_3^{\pm}\right) \\
&+ (\pm h)u_y + \left(\pm\tfrac{h}{2}\right)(\pm h)\, u_{xy} + \left(\pm\tfrac{h}{2}\right)^2(\pm h)\tfrac{u_{xxy}}{2!} + \left(\pm\tfrac{h}{2}\right)^3(\pm h)\tfrac{u_{xxxy}}{3!} + \left(\pm\tfrac{h}{2}\right)^4(\pm h)\tfrac{u_{xxxxy}}{4!}\left(\tfrac{1}{2}\xi_3^{\pm,\pm},\xi_3^{\pm}\right) \\
&+ (\pm h)^2\tfrac{u_{yy}}{2!} + \left(\pm\tfrac{h}{2}\right)(\pm h)^2\tfrac{u_{xyy}}{2!} + \left(\pm\tfrac{h}{2}\right)^2(\pm h)^2\tfrac{u_{xxyy}}{2!} + \left(\pm\tfrac{h}{2}\right)^3(\pm h)^2\tfrac{u_{xxxyy}}{3!2!}\left(\tfrac{1}{2}\xi_3^{\pm,\pm},\xi_3^{\pm}\right) \\
&+ (\pm h)^3\tfrac{u_{yyy}}{3!} + \left(\pm\tfrac{h}{2}\right)(\pm h)^3\tfrac{u_{xyyy}}{3!} + \left(\pm\tfrac{h}{2}\right)^2(\pm h)^3\tfrac{u_{xxyyy}}{2!3!}\left(\tfrac{1}{2}\xi_3^{\pm,\pm},\xi_3^{\pm}\right) \\
&+ (\pm h)^4\tfrac{u_{yyyy}}{4!} + \left(\pm\tfrac{h}{2}\right)(\pm h)^4\tfrac{u_{xyyyy}}{4!}\left(\tfrac{1}{2}\xi_3^{\pm,\pm},\xi_3^{\pm}\right) \\
&+ (\pm h)^5\tfrac{u_{yyyyy}}{5!}\left(\tfrac{1}{2}\xi_3^{\pm,\pm},\xi_3^{\pm}\right)
\end{aligned}
$$

When the above expansions are inserted into the summation of $D_x^h c^h$, canceled out all the terms but the remainders.

$$
D_x^h c^h_{i+\frac{1}{2},j} = \frac{h^2}{120}\left(\begin{array}{l}
-\left(\frac{3}{2}\right)^5\left(u_{xxxxx}\left(\xi_1^+,0\right)+u_{xxxxx}\left(\xi_1^-,0\right)\right)+\frac{5}{2^5}\left(u_{xxxxx}\left(\xi_2^+,0\right)+u_{xxxxx}\left(\xi_2^-,0\right)\right) \\
-\left(\frac{1}{2}\right)^5\left(\begin{array}{l}
\left(u_{xxxxx}+u_{xxxxy}+u_{xxxyy}+u_{xxyyy}+u_{xyyyy}+u_{yyyyy}\right)\left(\frac{1}{2}\xi_3^{+,+},\xi_3^+\right) \\
+\left(u_{xxxxx}-u_{xxxxy}+u_{xxxyy}-u_{xxyyy}+u_{xyyyy}-u_{yyyyy}\right)\left(\frac{1}{2}\xi_3^{+,-},\xi_3^-\right) \\
+\left(u_{xxxxx}-u_{xxxxy}+u_{xxxyy}-u_{xxyyy}+u_{xyyyy}-u_{yyyyy}\right)\left(\frac{1}{2}\xi_3^{-,+},\xi_3^+\right) \\
+\left(u_{xxxxx}+u_{xxxxy}+u_{xxxyy}+u_{xxyyy}+u_{xyyyy}+u_{yyyyy}\right)\left(\frac{1}{2}\xi_3^{-,-},\xi_3^-\right)
\end{array}\right) \\
+\frac{5}{2}\left(\left(u_{xxxxx}+u_{xxxyy}\right)\left(\xi_4^+,0\right)+\left(u_{xxxxx}+u_{xxxyy}\right)\left(\xi_4^-,0\right)\right)
\end{array}\right)
$$

Now, we prove the lemma.

$$
\begin{aligned}
\left|D_x^h c^h_{i+\frac{1}{2},j}\right| &\leq \max_{\tilde{\Omega},|\alpha|\leq 5}\left|\partial^\alpha u\right|\cdot\tfrac{h^2}{120}\left(2\cdot\left(\tfrac{3}{2}\right)^5+2\cdot\tfrac{5}{2^5}+4\cdot 6\cdot\left(\tfrac{1}{2}\right)^5+2\cdot 2\cdot\tfrac{5}{2}\right) \\
&= \tfrac{105}{4}\max_{\tilde{\Omega},|\alpha\leq 5|}\left|\partial^\alpha u\right|\cdot h^2
\end{aligned}
$$

References

[1] L. A. Caffarelli and G. Gilardi. Monotonicity of the free boundary in the two-dimensional dam problem. *Annali della Scuola Normale Superiore di Pisa-Classe di Scienze*, 7(3):523–537, 1980.

[2] A. J. Chorin. A numerical method for solving incompressible viscous flow problems. *Journal of computational physics*, 135(2):118–125, 1997.

[3] P.G. Ciarlet, B. Miara, and J. M. Thomas. *Introduction to Numerical Linear Algebra and Optimisation*. Cambridge Texts in Applied Mathematics. Cambridge University Press, 1989.

[4] A. Friedman. *Variational principles and free-boundary problems*. Courier Corporation, 2010.

[5] F. Gibou and C. Min. Efficient symmetric positive definite second-order accurate monolithic solver for fluid/solid interactions. *Journal of Computational Physics*, 231:3245–3263, 2012.

[6] I. Gustafsson. A class of first order factorization methods. *BIT*, 18:142–156, 1978.

[7] F. H. Harlow and J. E. Welch. Numerical calculation of time-dependent viscous incompressible flow of fluid with a free surface. *Physics of Fluids*, 8(3):2182?–2189, 1965.

[8] A. Iserles. *A First Course in the Numerical Analysis of Differential Equations*. Cambridge Texts in Applied Mathematics. Cambridge University Press, 1996.

[9] Z.-C. Li, H.-Y. Hu, S. Wang, and Q. Fang. Superconvergence of solution derivatives of the shortley–weller difference approximation to poisson's equation with singularities on polygonal domains. *Applied Numerical Mathematics*, 58(5):689–704, 2008.

[10] Y. T. Ng, H. Chen, C. Min, and F. Gibou. Guidelines for poisson solvers on irregular domains with dirichlet boundary conditions using the ghost fluid method. *Journal of Scientific Computing*, 41(2):300–320, 2009.

[11] C. S. Peskin. Flow patterns around heart valves. In *Proceedings of the Third International Conference on Numerical Methods in Fluid Mechanics*, pages 214–221. Springer, 1973.

[12] G. H. Shortley and R. Weller. The numerical solution of laplace's equation. *Journal of Applied Physics*, 9(5):334–348, 1938.

[13] J. C. Strikwerda. *Finite difference schemes and partial differential equations*. SIAM, 2004.

[14] L. Weynans. *A proof in the finite-difference spirit of the superconvergence of the gradient for the Shortley-Weller method*. PhD thesis, INRIA Bordeaux, 2015.

[15] D. Xiu and G. E. Karniadakis. A semi-lagrangian high-order method for navier–stokes equations. *Journal of computational physics*, 172(2):658–684, 2001.

[16] G. Yoon and C. Min. Analyses on the finite difference method by gibou et al. for poisson equation. *Journal of Computational Physics*, 280:184–194, 2015.

[17] G. Yoon and C. Min. Convergence analysis of the standard central finite difference method for poisson equation. *Journal of Scientific Computing*, 67(2):602–617, 2016.

[18] G. Yoon, C. Min, and S. Kim. A stable and convergent method for hodge decomposition of fluid-solid interaction. *https://arxiv.org/abs/1610.03195*, 2016.